Advances in Powertrains and Automotives, 2015, Vol. 1, No. 1, 24-33
Available online at http://pubs.sciepub.com/apa/1/1/3

DOI:10.12691/apa-1-1-3

Effect of Ambient Gradients on Sound Transmission in Narrow Permeable Rectangular Pipes with Application to Heat Exchangers

Sabry Allam*

Automotive Technology Department, Faculty of Industrial Education, Helwan University, Cairo, Egypt
*Corresponding author: allam@kth.se

Received April 30, 2015; Revised May 08, 2015; Accepted May 25, 2015

Abstract The effect of ambient gradients on sound propagation in air filled narrow tube was investigated. The narrow tubes were taken to be nominally straight with very small pores in the walls. The solution includes the effect of a static pressure, temperature and density gradients in the presence of mean flow, which is assumed to have a uniform velocity profile. A dispersion equation is derived by assuming the spatial variations of the ambient variables can be lumped by using their average values. The complex wave number, density, speed of sound and the characteristic impedance of such media were evaluated. An application to fulfil narrow tubes with rectangular cross section and permeable walls such as; heat exchangers is developed and presented. An accurate acoustic model based on two-port matrix to calculate the transmission losses in the heat exchanger (HE) taking the ambient gradients effects into account are developed and used to study and improve the acoustic performance of HE. The developed model is validated with the measured results using normal incident and diffuse field at room temperature and a good agreement is achieved. Based on the results presented in this paper, the acoustic performance of the existing heat exchanger is bad especially at low frequencies, the operating conditions have some positive effects on its performance and its acoustic performance can be improved through channel wall impedance. Extra improvements are still needed to use it as a passive noise control element to damp the fan noise.

Keywords: *sound transmission, narrow permeable pipes, normal incident and diffuse field measurement, wall impedance optimization and heat exchanger*

Cite This Article: Sabry Allam, "Effect of Ambient Gradients on Sound Transmission in Narrow Permeable Rectangular Pipes with Application to Heat Exchangers." *Advances in Powertrains and Automotives*, vol. 1, no. 1 (2015): 24-33. doi: 10.12691/apa-1-1-3.

1. Introduction

1.1. General

Acoustic wave propagation within a homogeneous thermo-viscous fluid-filled medium at rest, unbounded in all directions, involves reactive and absorbing processes, which can be characterized, in the frequency domain, by a complex wave number. The imaginary part of which is proportional to the shear and bulk viscosity coefficients and the heat conduction coefficient. It can also include dissipation processes due to molecular relaxation using the appropriate complex specific heat ratio [1].

In a bounded domain (duct or cavity), the reactive and absorbing processes at rigid boundaries arise from interactions between the acoustic movements and both the entropic movement (diffusion of heat) and the vortical movement (diffusion of shear waves), which are created on the boundary walls, extracting energy from the acoustic wave. The entropic and vortical perturbations diffuse into the medium in direction normal to the boundary, which is a consequence of the uniform boundary conditions, and die out before reaching the opposite wall. Provided that the local curvature and distance between the walls are large enough with respect to the boundary layer thicknesses. In these situations, the absorption of acoustic waves outside the boundary layers can be characterized, in the frequency domain, by the imaginary part of a complex wave number, which in most cases will be proportional to the square root of the shear viscosity coefficient as well as that of the heat conduction coefficient [1].

A somewhat different approach is needed in very small cavities and narrow ducts, where one or two of the dimensions are of similar magnitude to the boundary layer thicknesses. In these situations, which can be found in numerous acoustic devices (more particularly electroacoustic devices), the heat diffusion (entropic movement) and the shear wave diffusion (vortical movement) have amplitudes of the same order of magnitude as the acoustic wave itself (which acts on the wall as a source for the entropic and vortical movement). In these circumstances, the approach must involve a precise description of the particle movement inside the boundary layers.

This particle movement can be expressed in terms of a superposition of three kinds of components: first, the original wave (which provides energy), second, thermal and viscous dissipation in the form of correction factors

added to the acoustical wave function and third, diffusion of heat and shear waves also described by means of additive functions [1].

Over the last 2 decades, theoretical activities on the subject provide a relevant global formulation, which would be able to satisfy the requirements mentioned above for describing the acoustic fields in thermo-viscous fluids. In publications which relate to this subject one finds: (i) the pioneering works of Dokumaci [3], which lead to both a modelling of viscous boundary layers in a narrow circular and rectangular pipes by taking in his account the ambient gradients effect in the case of circular narrow pipes with the solid wall (ii) the works of Cummings for rectangular and square narrow ducts [5] and (iii) Peat et al [6], which uses numerical methods to model thin layers of viscous fluid trapped between parallel walls (iv) K.- W. JEONG etal [8] uses a numerical method to study the sound transmission in capillary tubes with mean flow. All of these papers assume that they have isothermal boundary condition and hard wall, very few work such as [10], have been introduced to implement the wall effect, in their work an average solution to the sound transmission in narrow pipes with porous wall is presented and applied to diesel particulate trap. Allam and Åbom [11] presented a simplified approach based an equivalent fluid model to study the sound transmission in HE, this model is primitive and based on the measured flow resistivity of the HE. So, the problem of sound waves propagation in narrow permeable rectangular pipes carrying mean flow with ambient gradient is not addressed yet.

Generally, the heat exchanger is a specialized device that assists in the transfer of heat from one fluid to the other. In some cases, a solid wall may separate the fluids and prevent them from mixing. In other designs, the fluids may be in direct contact with each other. In the most efficient heat exchangers, the surface area of the wall between the fluids is maximized while simultaneously minimizing the fluid flow resistance. Fins or corrugations are sometimes used with the wall in order to increase the surface area and to induce turbulence. Common appliances containing a heat exchanger include air conditioners, refrigerators, and space heaters. Heat exchangers are also used in chemical processing and power production. Perhaps the most commonly known heat exchanger is a car radiator, which cools the hot radiator fluid by taking advantage of airflow over the surface of the radiator [12].

There are also four different designs of heat exchangers: shell and tube, plate, regenerative, and intermediate fluid or solid. The most typical type of heat exchanger is the shell and tube design. This heat exchanger has multiple finned tubes. One of the fluids runs through the tubes while the other fluid runs over them, causing it to be heated or cooled. In the plate heat exchanger, the fluid flows through baffles. This causes the fluids to be separated by plates with a large surface area. This type of heat exchanger is typically more efficient than the shell and tube design [12]. The regenerative heat exchanger takes advantage of the heat from a specific process in order to heat the fluid used in the same process. These heat exchangers can be made with the shell and tube design or the plate design. The intermediate fluid or solid heat exchanger uses the fluids or solids within it to hold heat and move it to the other side in order to be released. This method is commonly used to cool gases while removing impurities at the same time.

The object of this paper is to develop an accurate acoustic model based on two-port matrix to study and improve the acoustic performance of the plate heat exchangers (HE) taking the ambient gradients effects into account, by solving the convective wave equation in narrow rectangular pipes with the relevant boundary conditions.

1.2. Structure of the Paper

This paper describes the effect of ambient gradients on the sound transmission in narrow rectangular permeable tubes carrying mean flow. An analytical solution to the problem is presented in section 2 and summary of the measurement setup and procedure is presented in section 3, the model is employed to study the acoustic performance of HE and compared with measured results at room temperature in section 4. Finally, conclusions and proposal for Future work is presented in Section 5.

2. Problem Formulation

2.1. Wave propagation in Narrow tubes

The governing equation for a perfect gas in a uniform narrow rectangular pipe can be written using the basic equations presented in [4]. Assuming the mean flow velocity profile to be uniform across the pipe cross-sectional area and axial flow velocity, temperature, pressure gradients are taken into account. The convective equations can be expressed, with $\exp(-i\omega t)$ time dependence assumed for the fluctuating quantities, where ω is the radian frequency, t is the time and i denotes the unit imaginary number, as follows. The momentum equation is;

$$\rho_o\left(-i\omega + v_o\frac{\partial}{\partial x}\right)v_x + \rho_o v_x\frac{dv_o}{dx} = -\frac{\partial p_j}{\partial x} + \mu\nabla_s^2 v_x, p = p(x) \quad (1)$$

The continuity equation is:

$$\left(-i\omega + v_o\frac{\partial}{\partial x} + \frac{dv_o}{dx}\right)\rho + v_x\frac{d\rho_o}{dx} + \rho_o\frac{\partial v_x(x,y,z)}{\partial x} = -\frac{\rho_o}{A}\int_A \nabla_\tau \cdot v_\tau(x,y,z)\,dy\,dz \quad (2)$$

Here, x denotes the pipe axis, $\rho = A^{-1}\int\rho(x,y,z)\,dydz$, $v_x = A^{-1}\int v_x(x,y,z)\,dydz$ are the cross-sectional averaged acoustic density and x component of particle velocity with Area A is cross - section averaged acoustic.

Application to Eq. (2) of the divergence theorem in the (x,y) plane gives

$$\left(-i\omega + v_o\frac{\partial}{\partial x} + \frac{dv_{oj}}{dx}\right)\rho + v_x\frac{d\rho_o}{dx} + \rho_o\frac{\partial v_x(x,y,z)}{\partial x} = -\frac{\rho_o}{A}\int_S n(y,z)\cdot v_\tau(x,y,z)\,dS \quad (3)$$

where S being the perimeter of a main pore having outward unit normal **n** and dS an element of perimeter.

In case of impermeable walls narrow pipes equation (3) reduce to

$$\left(-i\omega + v_o \frac{\partial}{\partial x} + \frac{dv_{oj}}{dx}\right)\rho + v_x \frac{d\rho_o}{dx} + \rho_o \frac{\partial v_x(x,y,z)}{\partial x} = 0 \quad (4)$$

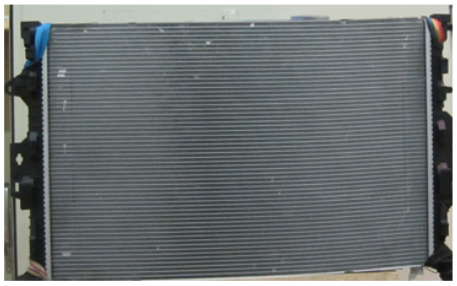

(a) Photo for car heat exchanger.

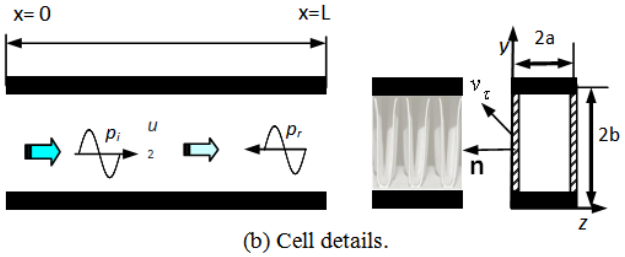

(b) Cell details.

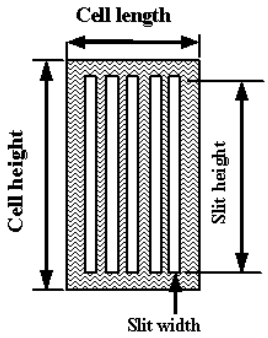

(c) Constructor drawing of cell wall shape

Figure 1. The geometry of a heat exchanger tubes

The energy equation when the perfect gas being assumed and neglecting the convective heat exchange with the channel walls, is

$$\rho_o C_p \left(-i\omega + v_o \frac{\partial}{\partial x}\right) T + \rho_o C_p v_x \frac{dT_{oj}}{dx} + \rho C_p v_o \frac{dT_{oj}}{dx} = \left(-i\omega + v_{oj} \frac{\partial}{\partial x}\right) p + v_x \frac{dp_o}{dx} + k_{th} \nabla_s^2 T. \quad (5)$$

The state equation is

$$\rho = \left(\frac{p}{RT_o}\right) - \left(\frac{\rho_o T}{T_o}\right), \quad (6)$$

While p, T and ρ is the acoustic pressure, temperature and average density respectively, μ is the shear viscosity coefficient. k_{th} is the thermal conductivity of the fluid, R is the gas constant, C_p is the specific heat coefficient at constant pressure. The mean flow velocity v_0 assumed to be axial and have velocity profile, the mean temperature T_o is assumed to be a function of the axial co-ordinate x. μ and k_{th} are the shear viscosity coefficient and thermal conductivity, respectively are assumed to be slowly varying function of T_o so that the gradients $\partial\mu/dx$ and $\partial\kappa_{th}/dx$ are small to the first order. The Laplacian on the cross-section ∇_s^2 and the divergence of the particle velocity $\nabla.v$ are given by

$$\nabla_s^2 = \frac{\partial^2}{\partial y^2} + \frac{\partial^2}{\partial z^2}, \nabla.v = \frac{\partial \upsilon_x}{\partial x} + \frac{\partial \upsilon_y}{\partial y} + \frac{\partial \upsilon_z}{\partial z} \quad (7)$$

where, y and z denote the transverse co-ordinates as shown in Figure 1, with the pipe cross-sectional area lying in, υ_y and υ_z are the components of the particle velocity in the y and z directions.

According to Eq. (3), the average gas density in the main tubes changes in time due to compression of the gas and as a result of mass flux $\rho_o n(x,y)\cdot v_\tau(x,y,z)$ into the pore wall. A reasonable assumption is that the permeable wall radius is too small compare to main tube and wave length λ » a (the duct hydraulic radius). Under this assumption the wall can be taken locally to be a flat surface having specific acoustic impedance Z_w. In this averaged sense continuity of the normal component of at the tube wall boundary is taken to be

$$n(x,y)\cdot v_\tau(x,y,z) = p(x)/Z_w \quad (8)$$

Here p is taken to be constant in a given cross section of a main pore. Use of the boundary condition, Eq. (7), in the continuity equation, Eq. (3), gives

$$\left(-i\omega + v_o \frac{\partial}{\partial x} + \frac{dv_{oj}}{dx}\right)\rho + v_x \frac{d\rho_o}{dx} + \rho_o \nabla.v + \rho_o \frac{S}{AZ_w} p \quad (9)$$

Recall again **S** is the perimeter of the arbitrarily shaped main pore which is shown in Figure 1. The axial distribution of the mean temperature and pressure is assumed to be linear and are expressed in the following forms

$$T_o(x) = \bar{T}_o(1+\tau\zeta), p_o(x) = \bar{p}_o(1+\varepsilon\zeta), \quad \zeta = -1 + 2x/L \quad (10)$$

where, p_o denotes the ambient pressure, L is the length of the pipe, the over bar (−) denotes an axial average, and the temperature change parameters are defined as

$$\tau = \frac{T_o(L) - T_o(0)}{2\bar{T}_o}, \varepsilon = \frac{p_o(L) - p_o(0)}{2\bar{p}_o} \quad (11)$$

Since the mean flow velocity in the transverse direction is too small compare to axial mean flow velocity, so the axial mean can be determined in the same way like the hard wall from the continuity equation for the mean flow, $\rho_o v_o$ = constant. The axial variation of the mean density distribution is then determined by the perfect gas law $p_o = \rho_o R T_o$. Hence, the ambient gradients, which occurring in the governing acoustic equations can be

expressed in terms of the temperature and pressure change parameters by using the following relations.

$$\frac{dT_o}{dx}=\frac{2\tau\bar{T}_o}{L},\frac{dp_o}{dx}=\frac{2\varepsilon\bar{p}_o}{L},\quad \frac{d\rho_o}{\rho_o dx}=\frac{dv_o}{v_o dx}=\frac{\bar{T}_o}{T_o}\frac{2\tau}{L}-\frac{\bar{p}_o}{p_o}\frac{2\varepsilon}{L} \tag{12}$$

Using these gradients (8), (9) and (10) and dropping the index j to avoid any disturbance equation (1), (2) and (3) can be expressed to $o\left(\tau^2\right)$ and $o\left(\pi^2\right)$ as follows

$$-\bar{\rho}_o i\omega\left[1-(\tau-\varepsilon)\zeta\right]v_x+\bar{\rho}_o\bar{v}_o\left[\frac{\partial v_x}{\partial x}+\frac{2(\tau-\varepsilon)v_x}{L}\right]= -\frac{\partial p}{\partial x}+\bar{\mu}\left(1+\frac{\tau\zeta}{2}\right)\nabla_s^2 v_x \tag{13}$$

Using equation (9), (10), and (11) with equation (4) yield

$$-\rho_0\bar{C}_p\left(i\omega\left[1-(\tau-\varepsilon)\zeta\right]T+\bar{v}_o\left\{\frac{2\tau T}{L}-\frac{\partial T}{\partial x}\right\}\right)= -\left(\varepsilon-\frac{\bar{\gamma}\tau}{\bar{\gamma}-1}\right)\frac{2\bar{p}_o v_x}{L}-\left[\begin{array}{l} i\omega p+\bar{v}_0\left\{\begin{array}{l}\frac{2\bar{\gamma}\tau p}{L(\bar{\gamma}-1)}-\\ \left[1-(\tau-\varepsilon)\zeta\right]\frac{\partial p}{\partial x}\end{array}\right.\end{array}\right] +\bar{k}_{th}\left(1+\frac{\tau\zeta}{2}\right)\nabla_0^2 T \tag{14}$$

Using the above-described approximation, the solution of equation (1), (2) and (3) can be searched in the form;

$$p=A\exp\left(i\Gamma k\ x\right),\upsilon_x=H(y,z)p,T=F(y,z)\,p \tag{15}$$

where, A denote any arbitrary constants. Substituting equations (15) in equations (13) and (14) yields

$$\frac{\partial^2 H}{\partial y^2}+\frac{\partial^2 H}{\partial z^2}+\beta^2 H\ =\beta_o^2 \tag{16}$$

and

$$\frac{\partial^2 F}{\partial y^2}+\frac{\partial^2 F}{\partial z^2}+\sigma^2 F=\left(\sigma_o^2\right)\ +\sigma_1^2 H\ \ (y,z) \tag{17}$$

where

$$\beta_o^2=\frac{i\Gamma\bar{k}}{\bar{\mu}},\sigma_o^2=\frac{i\omega}{\kappa_{th}}\left[1-\bar{M}\Gamma+\frac{2\tau\bar{M}\bar{\gamma}}{i(\bar{\gamma}-1)\bar{k}L}\right], \sigma_1^2=\frac{2\bar{p}_o}{\bar{\kappa}_{th}L}\left[\frac{\tau_j\bar{\gamma}}{(\bar{\gamma}-1)}-\varepsilon\right],(\beta a)^2=i\Phi(\varepsilon-\tau)s\bar{s}^2, \left(\sigma^2 a^2\right)=\left(i\Phi(\tau)\bar{s}^2\,\bar{\mathrm{Pr}}\right), \tag{18}$$

where,

$$\bar{k}=\frac{\omega}{\bar{c}},\bar{c}=\sqrt{\left(\frac{\bar{\gamma}\,\bar{p}_0}{\bar{\rho}_0}\right)},\bar{s}=a\sqrt{\frac{\bar{\rho}_o\,\omega}{\bar{\mu}}}, \bar{\mathrm{Pr}}=\frac{\bar{\mu}\bar{C}_P}{\bar{k}_{th}},\bar{M}=\left(\frac{\bar{v}_o}{\bar{c}}\right) \tag{19}$$

The function Φ is defined as

$$\Phi(\varepsilon)=1-\bar{M}\Gamma+\frac{2\bar{M}_j\varepsilon}{i\bar{k}L} \tag{20}$$

where, a halve of the monolith width, $\bar{M}$ is the average mean flow Mach number, $\bar{c}$ is the speed of sound, γ is the ratio of the specific heat coefficients, $\bar{k}$ is the wave number, $\bar{s}$ is the shear wave number, and $\bar{\mathrm{Pr}}$ is the average Prandtle number. The solution of the equation (16) can be expressed in the form of a double Fourier series [13].

$$H(y,z)=\Sigma_{m,n}\,h_{mn}\sin\left(\frac{\lambda_m y}{2a}\right)\sin\left(\frac{\lambda_n z}{2b}\right), \lambda_i=(2i+1)\pi,i=0,1,2,.. \tag{21}$$

The index i=m and n. The coefficient h_{mn} can be determined by substituting the equation (21) in equation (16) (the strategy of the solution is presented in the Appendix A), which yields

$$h_{mn}=\frac{16i\bar{k}\Gamma}{\bar{\mu}}\left(\frac{1}{\lambda_m\lambda_n\beta^2\alpha_{mn}(\beta a)}\right) \tag{22}$$

By inserting equation (22) in equation (21), H can be determined by integrating and averaging the resulting over the pipe cross-section area

$$H(y,z)=\Sigma_{m,n}\,h_{mn}\sin\left(\frac{\lambda_m y}{2a}\right)\sin\left(\frac{\lambda_n z}{2b}\right) \tag{23}$$

By integrating over the pipe area and after some math

$$\langle H\rangle=-\frac{\Gamma}{\Phi(\varepsilon-\tau)\rho_o\,\bar{c}}J(\beta a) \tag{24}$$

where

$$J(\beta a)=-64\Sigma_{m,n}\left(\frac{1}{\lambda_m^2\lambda_n^2\alpha_{mn}(\beta a)}\right) \alpha_{mn}(\beta a)=1-\frac{1}{4(\beta a)^2}\left(\lambda_m^2+\lambda_n^2\frac{a^2}{b^2}\right) \tag{25}$$

Also, the solution of the equation (17) can be also expressed in the form of a double Fourier series.

$$F(y,z)=\Sigma_{m,n}\ f_{mn}\sin\left(\frac{\lambda_m y}{2a}\right)\sin\left(\frac{\lambda_n z}{2b}\right) \tag{26}$$

The coefficient f_{mn} can be determined using the same technique and it presented in the Appendix B.

$$f_{mn}=\frac{16}{\lambda_m\lambda_n\sigma^2\alpha(\sigma a)}\left\{\sigma_o^2+\frac{\sigma_1^2\beta_o^2}{\beta^2\alpha(\beta a)}\right\} \tag{27}$$

By integrating over the tube area gives

$$\langle F\rangle=\frac{-\sigma_0^2}{\sigma^2}J(\sigma a)-\frac{\sigma_1^2}{\sigma^2}\frac{\beta_o^2}{\beta^2}\frac{J(\sigma a)}{\alpha_{mn}(\beta a)} \tag{28}$$

where $J(\sigma a) = -64\sum_{m,n}\left(\frac{1}{\lambda_m^2\lambda_n^2\alpha_{mn}(\sigma a)}\right)$.

Using equation (9), (10) ,(19) and (20) with (8) yield

$$i\bar{k}\left(I_1 - I_2 - I_3\right) = \rho_o \frac{S}{AZ_w}, \tag{29}$$

where

$$I_1 = \frac{\bar{c}}{\bar{p}_0}\{\Phi(\varepsilon)\}, I_2 = \left(\frac{\bar{c}}{\bar{T}_0}\{\Phi(\tau)\}F(y,z)\right) \tag{30}$$
$$and\ I_3 = \left(\left\{\frac{2(\varepsilon-\tau)}{i\bar{k}L}+\Gamma\right\}H(y,z)\right)$$

By integrating and take the average around the tube cross section gives

$$\frac{ik_o\Phi(\varepsilon)}{\rho_o}\{\gamma + C_1 I(\sigma a) + C_2 I(\sigma\beta a) + C_3 I(\beta a)\} = \rho_o\frac{S}{AZ_w} \tag{31}$$

where

$$C_1 = \rho_o\gamma R\frac{\Phi(\tau)}{\Phi(\varepsilon)}\frac{\sigma_0^2}{\sigma^2}, C_2 = \rho_o\gamma R\frac{\Phi(\tau)}{\Phi(\varepsilon)}\frac{\sigma_1^2}{\sigma^2}\frac{\beta_0^2}{\beta^2}, \tag{32}$$
$$and\ C_3 = \frac{\Gamma\left(\frac{2(\tau-\pi)}{i\bar{k}L}+\Gamma\right)}{\Phi(\varepsilon)\Phi(\varepsilon-\tau)}$$

Equation (32) is solved using Newton-Raphson method for Γ and sample of the results is shown in Figure (2)

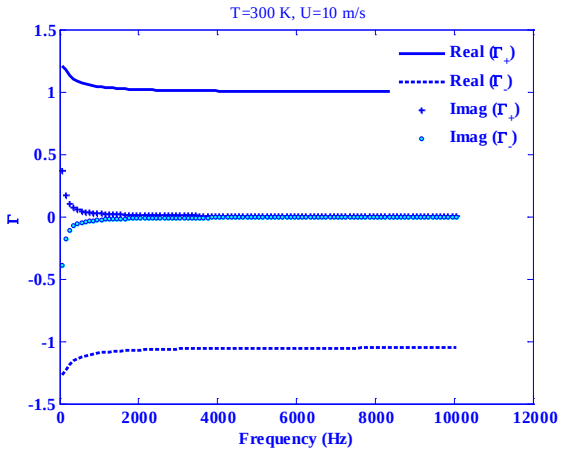

Figure 2. Propagation constants versus frequency at room temperature and flow speed 10 m/s. HE cell porosity σ=64%. Wall porosity = σ =0.5%. Cell dimension, (a=0.5, b=3.5, L=18) mm.

2.2. Slit-Shaped Perforated Wall Impedance

For this type of plates that shown in Figure 1 (c), Allard [14] gives an equation for the impedance of a slit

$$r_m = real\left(\frac{j\omega t}{\sigma c_o}\left[1-\frac{\tanh(\beta\sqrt{j})}{\beta\sqrt{j}}\right]^{-1}\right) + \frac{2\sqrt{2\eta\omega}}{\sigma c_o\omega} \tag{33}$$

and

$$\omega m = imag\left(\frac{j\omega t}{\sigma c_o}\left[1-\frac{\tanh(\beta\sqrt{j})}{\beta\sqrt{j}}\right]^{-1}\right) + \frac{\omega b}{2\sigma c_o}F(e) \tag{34}$$

where $\beta = \frac{b}{2}\sqrt{\rho_o\omega/\eta}$, b is the width of the slits, σ is the wall porosity (number of slits × area of slit/ slit wall area). By introducing an ellipticity factor e, l is the half length of slit. $e = \sqrt{1-(\frac{b}{l})^2}$, and $F(e) = \int_0^{\pi/2}\frac{d\theta}{\left(1-e^2\cos^2\theta\right)^{1/2}}$

Which can be expressed as a series becomes [4]:

$$F(e) = \frac{\pi}{2}\left(1+\frac{1^2}{2^2}e^2+\frac{1^2.3^2}{2^2.4^2}e^4+\frac{1^2.3^2.3^2}{2^2.4^2.6^2}e^6+\cdots\right) \tag{35}$$

Lists of value of l/b corresponding to the ellipticity e and corresponding *F(e)* are shown in Table 1.

Table 1. The mass end correction of an ellipse from Maa [15]

l/b	$e=\sqrt{1-(\frac{b}{l})^2}$	½ F(e)
2	0.86603	1.078
5	0.97980	1.508
10	0.99499	1.845
20	0.99815	2.192
50	0.99980	2.663
100	0.999949	2.988
200	0.999888	3.348
500	0.999996	3.792
1000	0.999999	4.016
2000	0.99999975	4.500

2.3. Sound Transmission Calculation

The sound transmission through the heat exchanger is most effectively handled using a transfer-matrix approach [2]. So, if only plane waves exist in a system with just two openings the system can be described as an acoustic two-port matrix. The most commonly used model is developed by using acoustic pressure p and velocity v to represent the input and output state vector. Using the boundary conditions at $x_1 = 0, L$ and the continuity of p and v, implies that we only have to analyze the reflection and propagation in the x_1 direction. A transfer matrix suited for this problem can be defined by:

$$\begin{pmatrix}\hat{p}\\ \hat{v}\end{pmatrix}_{x_1=0} = \begin{pmatrix}T_{11} & T_{12}\\ T_{21} & T_{22}\end{pmatrix}\begin{pmatrix}\hat{p}\\ \hat{v}\end{pmatrix}_{x_1=L}, \tag{36}$$

where T is given by [2]:

$$T = \begin{pmatrix}\cos(\Gamma kL) & \frac{i}{\langle H\rangle}\sin(\Gamma kL)\\ i\langle H\rangle\sin(\Gamma kL) & \cos(\Gamma kL)\end{pmatrix} \tag{37}$$

To obtain the acoustic transmission the boundary conditions and the plan wave relationships on the inlet and outlet sides with the help of equation (15) imply that:

$$\begin{cases} \hat{p}_{x_1=0} = \hat{p}_i + \hat{p}_r = \hat{p}_i(1+r) \\ \hat{v}_{x_1=0} = \hat{p}_i(1-r)\langle H \rangle \end{cases} \tag{38}$$

and

$$\begin{cases} \hat{p}_{x_1=L} = \hat{p}_t = \tau \cdot \hat{p}_i \\ \hat{v}_{x_1=L} = \hat{p}_t \langle H \rangle = \tau \cdot \hat{p}_i \langle H \rangle \end{cases} \tag{39}$$

where the amplitudes of the reflected and the transmitted fields are related to the incident wave with a transmission coefficient τ ($\tau = \hat{p}_t / \hat{p}_i$) and a reflection coefficient r ($r = \hat{p}_r / \hat{p}_i$). Substituting equations (38) and (39) into equation (36), yields

$$\begin{cases} 1+r = \tau\cos(\Gamma kL) + i\tau\sin(\Gamma kL) \\ 1-r = i\tau\sin(\Gamma kL) + \tau\cos(\Gamma kL) \end{cases} \tag{40}$$

By evaluating equation (40), the transmission and reflection coefficients can be obtained as

$$\tau = \frac{1}{\cos(\Gamma kL) + i\sin(\Gamma kL)} \tag{41}$$

The propagation constant Γ can be obtained from equation (31). Transmission loss *TL* for a certain incident angle (θ, φ) becomes

$$TL(\overline{n}_i) = 10\log\frac{1}{|\tau(\overline{n}_i)|^2}. \tag{42}$$

where $\overline{n}_i$ is the unit vector along the incidence direction. By averaging equation (42) over all possible incident angles, the transmission loss in a diffuse field is obtained [14]

$$\langle TL \rangle = -10\log\langle |\tau|^2 \rangle. \tag{43}$$

where

$$\begin{aligned} &\langle |\tau(\overline{n}_i)|^2 \rangle_{all\ \ angles} \\ &= \frac{1}{2\pi}\int_{\theta=0}^{\pi/2}\int_{\phi=0}^{2\pi} |\tau(\theta,\phi)|^2 \sin 2\theta \cdot d\theta d\phi. \end{aligned} \tag{44}$$

3. Summary of Experimental Procedure

3.1. 2-Port Experimental Procedure

Experiments were carried out at room temperature using the flow acoustic test facility at the Marcus Wallenberg Laboratory (MWL) for Sound and Vibration research at KTH. The test duct used during the experiments consisted of a standard steel-pipe with a wall thickness of 3 mm, duct inner diameter d_i=91 mm and overall length of around 7 meters. Four loudspeakers were used as external acoustic sources, and they were divided equally between the upstream and downstream side as shown in Figure 3. The distances between the loudspeakers were chosen to avoid any pressure minima at the source position. Six flush mounted condenser microphones (B&K 4938) were used, three upstream and three downstream of the test object for the plane wave decomposition, the microphone separations are chosen to fulfill the frequency ranges of interest up to 1 KHz.

All measurements are performed using the source switching technique [17] and the flow speed was measured upstream of the test section using a small pitot-tube fixed at a distance of 1000 mm from the upstream loudspeakers section and connected to an electronic manometer at SWEMA AIR 300. The pressure drop across each sample is also measured in using the same electronic manometer.

Three different errors can be occurred (i) the errors in the measured input data; (ii) the error sensitivity of the plane wave decomposition and (iii) the error sensitivity of the matrix equation. Point (i) and (ii) have been discussed in [18] and concluded that to obtain good measurement results, the plane wave decomposition must be restricted to the frequency range

$$0.1\pi\left(1-M^2\right) < ks < 0.8\pi\left(1-M^2\right) \tag{45}$$

Where k is the wave number and s is the microphone separation. Regarding point (iii) it will mainly depend on the inversion of the matrix. When this matrix is singular; or almost singular, large errors can be expected. To avoid this, the two test states for the two-port must be significantly different. All these precautions have been taken into account to avoid any measurement errors.

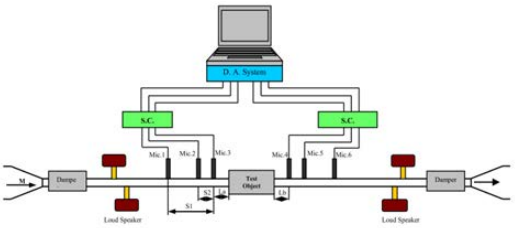

(a) Schematic drawing of the experimental setup.

(b) Samples of the used test object.

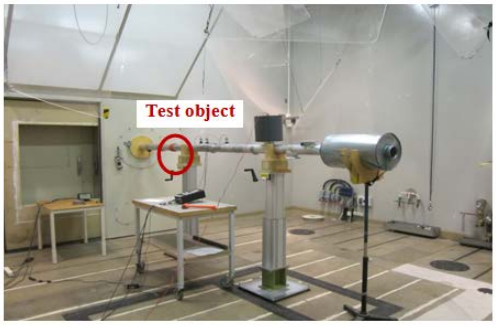

(c) Photo of test rig.

Figure 3. Measurement set up used during the 2- Port Experimental procedure

3.2. ISO 15186 Experimental Procedure

In this procedure, the object is treated as a wall element and the sound source emitting white noise was mounted in the reverberation room and the sound reduction index can be measured with ISO 15186-1:2000 [19]:

$$TL = L_{Sp} - 6 - L_{SI} + 10\log(A_m / A) \qquad (46)$$

where L_{Sp} is the sound pressure level measured by a rotating microphone in the reverberation room and L_{SI} is the sound intensity level obtained by scanning the surface of the heat exchanger with an intensity probe (**L.D. 2800**) in the receiving anechoic room. The whole setup can be seen in Figure 4. Here, A_m is the total area of the measurement surface and A is the area of the test specimen under test, and in these measurements the scanning is done overall the test specimens.

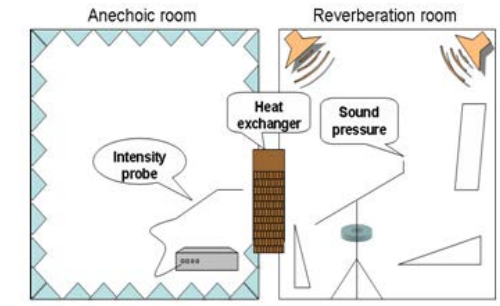

(a) Layout of the measurement procedure.

(b) Photo of the measurement procedure.

Figure 4. Measurement setup used with ISO standard (15186 -1:2000) procedure

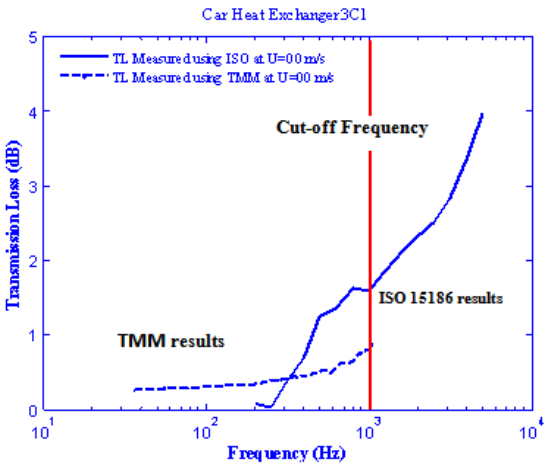

Figure 5. Difference in measured TL using ISO and TMM. HE dimensions (430× 400 × 140) mm, cell porosity σ=64%

3.3. Comparison between Results from Two Measurement Methods

Due to the difference between the normal incidence that is used with 2-port measurement and oblique incidence plane wave, which is used with ISO 15186, one can notice that there is deference between the measured results as shown in Figure 5. This difference is found to be between (1- 1.5) dB in most of the measured cases.

4. Results and Discussion

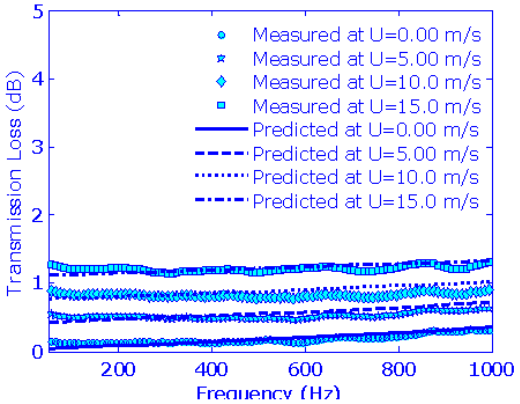

(a) Normal incident sound region.

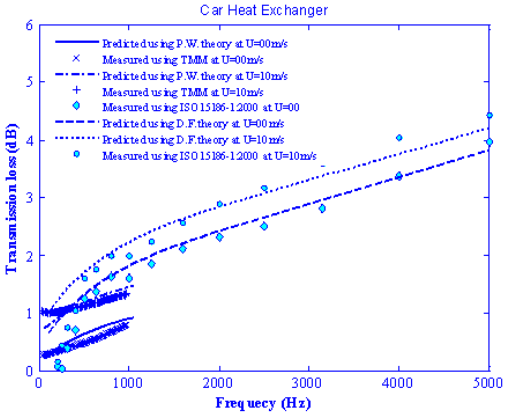

(b) Normal incident and diffuse sound field regions.

Figure 6. Transmission loss in one third octave band versus frequency. HE Dimensions (680× 470 × 18) mm, cell porosity σ=64%. Wall porosity = σ =0.5%, T_o = 300 K, τ=0.

The developed model presented in section 2, is used to calculate the sound transmission loss in heat exchangers for both normal incident sound field (where θ =0, and φ=0) and diffuse sound field. *Figure 6* shows the transmission loss for a sample of an automotive heat exchanger at two different flow speeds (U=0, and 10 m/s) at room temperature. It can be seen from the results, the model give a good agreement with the measured results in both normal incident and diffuse sound fields. It can be also noted that sound transmission loss of the Heat exchanger is very small especially at low frequency, then keywords to improve the heat exchanger acoustic performance though the pipes wall permeability i.e. through wall impedance and heat exchanger wall thickness. The wall impedance can be improved using different wall porosity, material and wall thickness. But, these parameters are critical because they are affect the thermal performance of the heat exchangers and the pressure drop, in other words

some kind of nonlinear multi-object optimization is needed to improve the heat exchanger performance and use it to as acoustic element as well as thermal element. The effect of flow speed on HE pressure drop is very small as shown in Figure 7, this due to its short length and cell opening porosity, which is σ=64% but it can be reduced or at least kept constant during redesigning and optimization process.

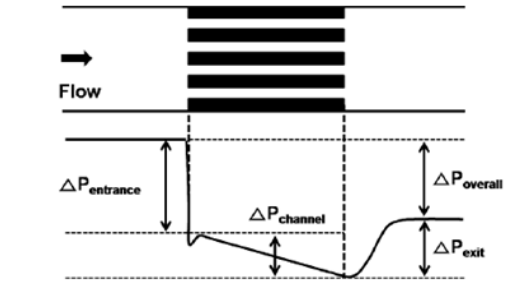

(a) Schematic drawing for relationship between flow and pressure drop diagram.

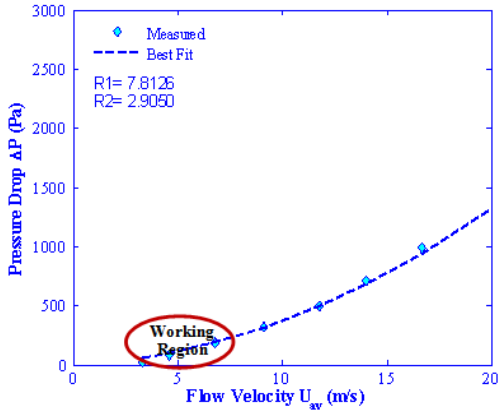

(b) Measured pressure drop

Figure 7. Pressure drop versus flow speed at room temperature.

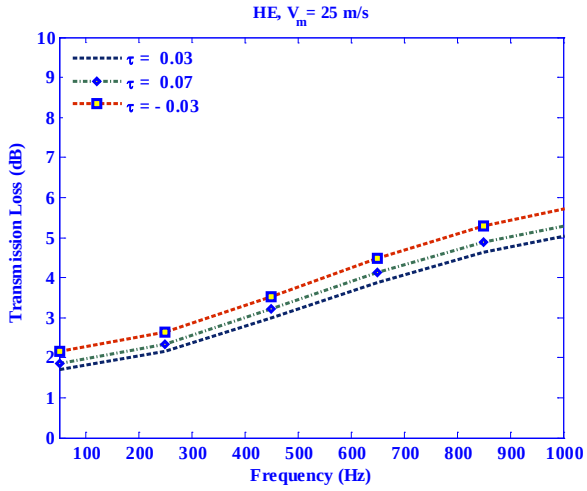

Figure 8. Transmission loss in one third octave band versus frequency. HE Dimensions (680 × 470 × 18) mm, cell porosity σ=64%. Wall porosity = σ =0.5%. T_O = 330 K.

Comparing Figure 8 and Figure 7, it can notice that the operating conditions have big effects of acoustic performance of HE. This is basically comes from the effect of operating conditions on the air density and speed of sound. It can be also, notice from Figure 8 that flow direction has some effect. It can be mentioned that flow direction depends on type of unit; movable (plus direction) or stationary (negative direction).

The effect of designing parameters such as wall impedance, cell dimension and porosity can be used as examples to improve the acoustic performance of HE. The effect of wall porosity on the sound transmission loss is presented in Figure 9, it can be seen that TL direct proportional to the wall porosity, but to avoid its effect on the thermal performance a full optimization process should be done.

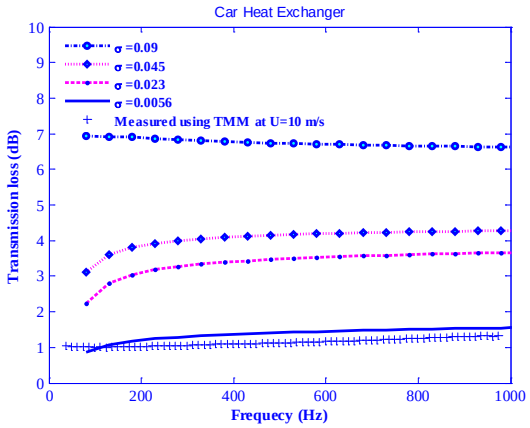

Figure 9. Effect of wall porosity on transmission loss. Cell porosity, σ=64%, U=10 m/s, T_O = 300 K, τ=0.

5. Conclusion and Future work

In this paper, an approximate solution to sound transmission in narrow tubes carrying mean flow with ambient gradients is presented. The developed model is employed to study the acoustic performance of the heat exchanger aiming at introducing it as an acoustic element for fan passive noise control and it has been examined both experimentally and theoretically.

The experimental assessment has been performed using two different methods; modified version of ISO 15186-1:2000 and the acoustic Two-Microphone Method (TMM). Theoretically, the basic configuration is assumed to be a matrix of parallel and rectangular narrow permeable channels. The developed model is based on quasi 3D wave propagation in narrow pipe with permeable boundary. Different results to characterize the acoustic performance of the heat exchanger are presented. From these results it is clear that the sound reduction in the existing HE is quite poor typically less than 5 dB up to 2-3 kHz and it can be improved using the developed model. The operating conditions have some positive sign effects on its performance.

Still an interesting question is therefore if, with unchanged thermal efficiency and pressure drop, one can improve the acoustic performance by introducing wall perforations with optimum impedance.

Acknowledgement

Part of this work has been financed by EU commission Grant Agreement no: SCP8-GA-2009-233541-ECOQUEST. The technical and scientific support from Mats Åbom from KTH, Sweden and Manuel Henner, from Valeo, France are beyond of my estimation.

References

[1] R. Bossart ,N. Joly and M. Bruneau “Hybrid numerical and analytical solutions for acoustic boundary problems in thermo-viscous fluids” Journal of Sound and Vibration 263 (2003) 69-84.

[2] Alland Pierce “Acoustic” Mc Graw-Hill, Inc. copyright 1981.

[3] E. Dokumaci “ On Transmission of Sound in Circular and Rectangular Narrow Pipes with Superimposed Mean Flow” journal of sound and vibration (1998) 210 (3), 375-389.

[4] E. Dokumaci “AN APPROXIMATE DISPERSION EQUATION FOR SOUND WAVES IN A NARROW PIPE WITH AMBIENT GRADIENTS” Journal of Sound and vibration (2001) 240(4), 637-646.

[5] R. J. ASTLEY and CUMMINGS “Wave propagation in catalytic converter: Formulation of the problem and finite element scheme. Journal of Sound and vibration (1995) 188(5), 635-657.

[6] K. Peat “A first approximation to the effects of mean flow on sound propagation tin capillary tubes” Journal of Sound and Vibration (1994) 475-489.

[7] K. Peat “Convected acoustic wave motion along A Capillary Duct with an axial temperature gradient” Journal of Sound and Vibration (1997) 203 (5) 855-866.

[8] K.-W JEONG and J.-G IH “A numerical study of the propagation of sound through capillary tubes with mean flow” Journal of Sound and Vibration (1996) 198 15) 67-79.

[9] N. Dickey, A. Selamet, J. Novak “Multi-pass perforated tube silencers: A computational approach” Journal of Sound and Vibration (1998) 211(3), 435-448.

[10] Sabry Allam and Mats Åbom “Sound Propagation in An Array of Narrow Porous Channels with Application to Diesel Particulate Filters” Journal of Sound and Vibration Vol. 291, (2006), 882-901.

[11] Sabry Allam and Mats Åbom “Acoustic Modelling and Characterization of Plate Heat Exchangers“. SAE Paper 2012-01-1562.

[12] Ramesh K. Shah and Dusan P. Sekulic; 2003 by John Wiley & Sons, Inc. Fundamentals of Heat Exchanger Design.

[13] L.S. Han “ Hydrodynamic Entrance Lengths for Incompressible Laminar flow in Rectangular Duct” Journal of Applied Mathematics, Transactions of ASME, September, 1960, 403-409.

[14] Allard, J. F., 1993, Propagation of Sound in Porous Media, Modelling Sound Absorbing Materials, Elsevier Applied Science, London.

[15] D. Y. Maa, “Potential of Micro-perforated panel absorber”, J. Acoust. Soc. Am. 104, 2861-2866 (1998).

[16] L.R.Koval 1976. The Journal of the Acoustical Society of America 59, 1379-1385. Effect of air flow, panel curvature and internal pressurization on field-incidence transmission loss.

[17] Mats Åbom. “Measurement of the Scattering-Matric of Acoustical Two-Ports”. Mechanical Systems and Signal Processing (1991) 5(2), 89-104.

[18] Hans Bodén and Mats Åbom “Influence of errors on the two-microphone method for measuring acoustic properties in ducts”. J. Acoust. Soc. Am. 79, 541 (1986).

[19] ISO 15186-1:2000 Acoustics - Measurement of sound insulation in buildings and of building elements using sound intensity - Part 1: Laboratory measurements.

Appendix A

The coefficient h_{mn} can be determined by substituting the equation (21) in equation (16) and the solution can discuss as follow

$$\Sigma_{m,n} h_{mn}\left(-\left(\frac{\lambda_m}{2a}\right)^2\right)\sin\left(\frac{\lambda_m y}{2a}\right)\sin\left(\frac{\lambda_n z}{2b}\right) + \Sigma_{m,n} h_{mn}\left(-\left(\frac{\lambda_n \pi}{2b}\right)^2\right)\sin\left(\frac{\lambda_m y}{2a}\right)\sin\left(\frac{\lambda_n z}{2b}\right) + \Sigma_{m,n} h_{mn}\left(\beta^2\right)\sin\left(\frac{\lambda_m y}{2a}\right)\sin\left(\frac{\lambda_n z}{2b}\right) = \left(\frac{i\bar{k}\Gamma}{\bar{\mu}}\right) \quad \text{A1}$$

Simplifying equation (A1) yields

$$\Sigma_{m,n} h_{mn}\left(\begin{array}{l}\beta_j^2 \\ -\left(\frac{\lambda_m}{2a}\right)^2 \\ -\left(\frac{\lambda_n}{2b}\right)^2\end{array}\right)\sin\left(\frac{\lambda_m y}{2a}\right)\sin\left(\frac{\lambda_n z}{2b}\right) = \left(\frac{i\bar{k}\Gamma}{\bar{\mu}}\right) \quad \text{A2}$$

Integrating and simplifying

$$\Sigma_{m,n} h_{mn}\beta^2\left(1-\frac{\pi^2}{4(\beta a)^2}\left(\lambda_m{}^2+\lambda_n{}^2\frac{a^2}{b^2}\right)\right) \sin\left(\frac{\lambda_m y}{2a}\right)\sin\left(\frac{\lambda_n z}{2b}\right) = \left(\frac{i\bar{k}\Gamma}{\bar{\mu}}\right) \quad \text{A3}$$

By putting $\alpha_{mn}(\beta a)=\left(1-\frac{\pi^2}{4(\beta a)^2}\left(\lambda_m{}^2+\lambda_n{}^2\frac{a^2}{b^2}\right)\right)$

in equation (A3) yields

$$\Sigma_{m,n} h_{mn}\beta^2\alpha(\beta a)\sin\left(\frac{\lambda_m y}{2a}\right)\sin\left(\frac{\lambda_n z}{2b}\right) = \left(\frac{i\bar{k}\Gamma}{\bar{\mu}}\right) \quad \text{A4}$$

By solving equation (A5) and using the advantage of the of the orthogonality according to [13]

$$h_{mn}\beta^2\alpha(\beta a)\,a\,b = \left(\frac{i\bar{k}\Gamma}{\mu}\right)\left(\frac{16ab}{\lambda_m\lambda_n}\right) \quad \text{A5}$$

which yields;

$$h_{mn} = \frac{16i\bar{k}\Gamma}{\bar{\mu}}\left(\frac{1}{\lambda_m\,\lambda_n\,\beta^2\alpha_{mn}(\beta a)}\right) \quad \text{A6}$$

Appendix B

Also, the solution of the equation (17) can also be expressed in the form of a double Fourier series, and the coefficient b_{mn} can be determined by substituting the equation (24), and (25) in equation (26), using the same technique and the final result can be expressed;

$$F(y,z) = \Sigma_{m,n}\, f_{mn}\sin\left(\frac{\lambda_m y}{2a}\right)\sin\left(\frac{\lambda_n z}{2b}\right), \quad m,n = 1,3,5,,... \quad \text{B1}$$

and

$$f_{mn} = \frac{16\sigma_o^2}{\lambda_m\,\lambda_n\left(\alpha^2-\frac{\lambda_m^2}{4a^2}-\frac{\lambda_n^2}{4b^2}\right)} + \frac{\sigma_1^2 h_{mn}}{\left(\alpha^2-\frac{\lambda_m^2}{4a^2}-\frac{\lambda_n^2}{4b^2}\right)} \quad \text{B2}$$

Simplifying equation B3 yields

$$f_{mn} = \frac{16}{\lambda_m \lambda_n \sigma^2 \alpha(\sigma a)} \left\{ \sigma_o^2 + \frac{\sigma_1^2 \beta_o^2}{\beta^2 \alpha(\beta a)} \right\} \quad \text{B3}$$

By inserting equation (B3) and equation (A7), F can be determined by integrating and averaging the resulting over the pipe cross-section area; as follow;

$$F(y,z) = \sum_{m,n} \frac{16}{\lambda_m \lambda_n \sigma^2 \alpha(\sigma a)} \left\{ \sigma_o^2 + \frac{\sigma_1^2 \beta_o^2}{\beta^2 \alpha(\beta a)} \right\} \times \sin\left(\frac{\lambda_m y}{2a}\right) \sin\left(\frac{\lambda_n z}{2b}\right) \quad \text{B4}$$

and

$$\langle F \rangle = \frac{-\sigma_0^2}{\sigma^2} J(\sigma a) - \frac{\sigma_1^2}{\sigma^2} \frac{\beta_o^2}{\beta^2} \frac{J(\sigma a)}{\alpha_{mn}(\beta a)} \quad \text{B5}$$